Coupling of porcine bone blood flow and metabolism in high-turnover bone disease measured by [^{15}O]H_2O and [^{18}F]fluoride ion positron emission tomography

Morand Piert[1], Hans-Jürgen Machulla[2], Michael Jahn[3], Anke Stahlschmidt[2], Georg A. Becker[2], Tilman T. Zittel[3]

[1] Nuclear Medicine, Klinikum rechts der Isar, Technical University of Munich, Ismaninger Strasse 22, 81675 München, Germany
[2] Radiopharmacy Section, PET Center, University of Tübingen, Germany
[3] Department of Abdominal and Transplantation Surgery, University of Tübingen, Germany

Received 24 November 2001 and in revised form 9 February 2002 / Published online: 13 April 2002
© Springer-Verlag 2002

Abstract. Previously, we identified a parathyroid hormone-related high-turnover bone disease after gastrectomy in mini pigs. Dynamic [^{18}F]fluoride ion positron emission tomography (PET) revealed that bone metabolism was significantly increased, but that bone blood flow derived from permeability-surface area product (PS product)-corrected K_1 values was not. Since bone blood flow and metabolism are coupled in normal bone tissues, we hypothesised that the capillary permeability and/or surface area might be altered in high-turnover bone disease. The "true" bone blood flow (f_{H2O}) was measured in vertebral bodies by dynamic [^{15}O]H_2O PET, followed by a 120-min dynamic [^{18}F]fluoride ion PET study, 6 months after total gastrectomy (n=5) and compared with results in sham-operated animals (n=5). Estimates for bone blood flow based on PS-corrected K_1 values (f) and the net uptake of fluoride in bone tissue (K_i), representing the bone metabolic activity, were calculated using standard compartmental modelling and non-linear fitting. Gastrectomy was followed by a significant elevation of K_i and k_3 (P<0.05), which was mainly caused by an increase of the fraction of bound tracer in tissue (P<0.01). In contrast, f_{H2O}, f, the single-pass extraction fraction of [^{18}F]fluoride (E) and the volume of distribution (DV) of [^{18}F]fluoride were not significantly different between groups. In both groups, a coupling of the mean f_{H2O} and K_i values was found, but the intercept with the y-axis was higher in high-turnover bone disease. It is concluded that in high-turnover bone disease following gastrectomy, the PS product for [^{18}F]fluoride remains unchanged. Therefore, even in high-turnover bone diseases, [^{18}F]fluoride ion PET can provide reliable blood flow estimates (f), as long as a proper PS product correction is applied. The increased bone metabolism in high-turnover bone disease after gastrectomy is mainly related to an up-regulation of the amount of ionic exchange of [^{18}F]fluoride with the bone matrix, while tracer delivery remains unchanged.

Keywords: Bone blood flow – Emission computed tomography – Fluorine-18 fluoride ion transport – Oxygen-15 water – High-turnover bone disease

Eur J Nucl Med (2002) 29:907–914
DOI 10.1007/s00259-002-0797-2

Morand Piert (✉)
Nuclear Medicine, Klinikum rechts der Isar,
Technical University of Munich, Ismaninger Strasse 22,
81675 München, Germany
e-mail: m.piert@lrz.tu-muenchen.de
Tel.: +49-89-41402970, Fax: +49-89-41404950

Introduction

Previously, bone disorders like osteomalacia and osteoporosis in excess of that associated with normal aging have been identified after gastrectomy and referred to as "postgastrectomy bone disease" [1, 2, 3]. This condition is characterised by a decreased bone mass and is associated with a considerably increased risk of vertebral bone fractures [4, 5, 6].

Recently, we were able to identify a high-turnover bone disease after gastrectomy in an established mini pig model. In this study, the increased bone metabolism was associated with significant bone loss, possibly due to secondary hyperparathyroidism [7]. It has been recognised for some time that bone blood flow and bone formation are linked under various physiological (growing skeleton, mature skeleton) and pathophysiological conditions (fractures, thyrotoxicosis) [8]. Using [^{18}F]fluoride ion positron emission tomography (PET) in combination with histomorphometric analyses, we have recently shown that bone blood flow and bone formation are coupled in normal bone tissue of mini pigs [9]. Nevertheless, the increase in bone metabolism after gastrectomy

was not accompanied by a similar increase in bone blood flow [7]. Therefore, these results indicated that the relationship between bone blood flow and metabolism might be specifically altered in high-turnover bone diseases.

In the aforementioned study, bone blood flow was not directly measured. Instead, bone blood flow was estimated by *f*, a permeability-surface area product (PS product)-corrected parameter derived from K_1 values obtained by [^{18}F]fluoride ion PET. The PS product used to estimate *f* (0.25 ml/[min×cm^3]) was derived from healthy mini pigs of the same age range [10]. Therefore, an increase in the extraction fraction due to an increase in the capillary permeability and/or capillary surface (dilatation of existing capillaries or recruitment of additional capillaries) in high-turnover bone disease might explain the discordance between bone blood flow and metabolism in high-turnover bone disease after gastrectomy. This would necessitate a disease-related PS correction factor and would complicate bone blood flow estimations based on [^{18}F]fluoride ion PET. On the other hand, if bone blood flow is indeed not increased in mild to moderate high-turnover bone diseases, our previous findings could only be explained if the amount of [^{18}F]fluoride ion undergoing ionic exchange with the bone matrix, and thus the fraction of bound tracer in tissue, increases. If this were the case, an up-regulation of osteoblast and osteoclast functions might be the underlying cause for the observed metabolic changes in high-turnover bone disease after gastrectomy.

In order to further elucidate the relationship of bone blood flow, fluoride ion extraction and bone metabolism, we performed a dual-PET tracer study with [^{18}F]fluoride ion and [^{15}O]H_2O 6 months after gastrectomy and compared the results with findings in healthy control animals. The study design allowed us to investigate whether bone blood flow and/or the [^{18}F]fluoride ion extraction, and thus the PS product, changes in high-turnover bone disease. Also, we were able to define the relationship between the "true" bone blood flow and bone metabolism in normal and high-turnover bone.

Materials and methods

Animals. Ten adult female mini pigs (Versuchstiergut Relliehausen, University of Göttingen, Göttingen, Germany) were used. The experimental conditions (animal housing environment, water and food intake) were the same as described previously [7, 9]. Briefly, the animals were accustomed to their new environment, and fed with a standard diet containing a defined amount of minerals and vitamin D (Altromin, Lage, Germany). Five animals were gastrectomised and received 1,000 µg vitamin B_{12} i.m. every 3 months, beginning 1 month after the operation, to avoid vitamin B_{12} deficiency. The control group was recruited from a group of seven mini pigs investigated earlier [10]. Out of these seven animals, two were excluded to account for the lower age of the five gastrectomised animals and to avoid possible errors in statistical analyses due to differing sample sizes of the two groups. The experimental protocol was reviewed and approved by the Animal Research Committee of the Administrative District of Tübingen. The institutional guidelines for the care and use of laboratory animals were followed throughout the study.

Surgery. All surgical procedures were performed after tracheal intubation under general anaesthesia, as previously described [2]. Briefly, a polyurethane catheter was implanted into the cephalic vein or external jugular vein as a central line to allow substitutions of fluids, electrolytes and calories for 5 days (Aminomix 1 500 ml/day, Fresenius, Bad Homburg, Germany and Sterofundin HEG-5 500 ml/day, Braun, Melsungen, Germany). The catheter was tunneled subcutaneously and brought out at the animal's back between the shoulder blades to avoid dislocation and infection. After gastrectomy, a Roux-Y reconstruction was performed (*n*=5). In the control group (*n*=5), the abdomen was opened without further manipulations to the intestinal tract (sham operation). All animals received cefuroxim (15 mg/kg body weight, Hoechst, Frankfurt, Germany) perioperatively.

Laboratory tests. Serum calcium, phosphate, haemoglobin, albumin and total protein were measured with standard methods as described previously [6]. Serum calcium was corrected for albumin and total protein as described elsewhere [11]. The fluoride serum level (unlabelled) was measured prior to tracer injection with an ion-sensitive electrode method. Parathyroid hormone (PTH) was measured by a two-site chemiluminometric sandwich immunoassay, which recognises intact parathyroid hormone (Magic Lite Intact PTH Immunoassay, Ciba Corning, Fernwald, Germany). The vitamin D metabolites, 25(OH)-vitamin D and 1,25$(OH)_2$-vitamin D, were measured by radioimmunoassay and by radioreceptor assay, respectively (Nichols Institute Diagnostics, San Juan Capistrano, Calif., USA). Bone-specific alkaline phosphatase was determined by an enzyme immunoassay (Alkphase-B, DPC Biermann, Bad Nauheim, Germany).

Radiotracer. [^{18}F]fluoride was produced via the ^{18}O(p,n)^{18}F nuclear reaction in a cyclotron (PETtrace, General Electric, Neu Isenburg, Germany) by irradiating 1.5 ml of ^{18}O-water (97% enrichment) with 16.5-MeV protons. The production yields were 2,200± 100 MBq/µAh at end of beam. [^{18}F]Fluoride was diluted in 10 ml of 0.9% saline solution for intravenous injection. The radiochemical purity of [^{18}F]fluoride was always >99% as determined by thin-layer chromatography (silica gel, Merck; CH_3CN:H_2O 95:5 (v/v); R_f =0).

Oxygen-15 was produced by bombardment of a mixture of 0.2% oxygen in $^{14}N_2$ (d,n) ^{15}O gas with 8.5-MeV deuterons. [^{15}O]H_2O was prepared by the reaction of oxygen with hydrogen in the presence of Pd as catalyst. After purification, the aqueous [^{18}F]fluoride and [^{15}O]H_2O solutions were passed through a 0.22-µm filter for sterilisation. The solutions were found to be pyrogen free (LAL-5000, Pyroquant Diagnostic, Germany).

Data acquisition. PET scanning was performed on an Advance PET scanner (General Electric Medical Systems, Milwaukee, Wis., USA) under general anaesthesia as described recently [9]. To allow arterial blood sampling, an arterial line was placed into the descending aorta via the femoral artery. For tracer injections and fluid substitutions (500 ml NaCl 0.9%), the cephalic vein was cannulated. After positioning, a 20-min transmission scan using a pair of rotating germanium-68 sources was performed. A bolus of approximately 30 MBq/kg body weight of [^{15}O]H_2O was injected. Simultaneously, a 10-min dynamic emission sequence of 45 PET scans was started according to the following protocol: 24×5 s, 12×10 s, 6×30 s, 3×60 s. After the complete decay of the [^{15}O]H_2O activity, a bolus of approximately 10 MBq/kg body weight of [^{18}F]fluoride ion was injected and the 120-min [^{18}F]fluoride ion PET scan followed (protocol: 12×10 s, 6×30 s, 5×5 min, 9×10 min). Arterial

blood samples were drawn continuously at a flow rate of 15 ml/min from the aorta by a calibrated infusion pump system (IMED Corporation Gemini PC-1, San Diego, Calif., USA) for the first 3 min of both scans. In previous experiments, this high flow rate had been found to produce undispersed input functions [10]. Whole blood radioactivity was measured continuously with a calibrated NaI detector system (Blood Sampler FRQ, Neu Isenburg, Germany). For the remaining scan time (after 3 min), blood samples were drawn discontinuously into heparinised syringes according to the scanning protocol. Plasma was separated from blood samples containing [^{18}F]fluoride and the radioactivity was counted in a calibrated NaI scintillation counter in order to obtain the distribution of [^{18}F]fluoride ion in plasma and whole blood.

Data analysis. Image analysis was performed on Apollo 9000 Model 735 workstations (Hewlett Packard, Palo Alto, Calif., USA) were reconstructed by filtered back-projection, employing a Hanning filter and corrected for attenuation and deadtime, resulting in 128×128 pixel images for the entire dynamic sequence. Standardised elliptical regions of interest (ROI size: 1.1 cm^2) were drawn in five or six vertebral bodies of each animal, selecting the mid-slice of each available vertebra in [^{18}F]fluoride PET images. The ROIs were then transferred to the corresponding [^{15}O]H_2O images. Sagittal and coronal image reconstructions of the last [^{18}F]fluoride image frame were performed to ensure correct ROI selection.

Mathematical models. Kinetic parameters were estimated from the tissue and arterial blood/plasma time-activity curves by a standard non-linear least-squares analysis using the Matlab Version 4.2 computing environment (The MathWorks Inc., Natick, Mass., USA) on a Sun Spark Ultra 10 workstation (Sun, Munich, Germany). For dynamic [^{15}O]H_2O PET studies, kinetic parameter estimations were derived from tissue and arterial whole blood activity curves of the first 5 min using a single tissue compartment model according to the Kety-Schmid method [12].

For [^{18}F]fluoride ion PET studies, the kinetic parameters were estimated from the tissue and arterial plasma activity curves according to a standard two-tissue compartment tracer kinetic model configuration [13]. The net uptake of fluoride in bone tissue, the macroparameter K_i, was calculated from individually fitted rate constants (K_i=K_1×k_3/(k_2+k_3) in ml/[min×cm^3]). The net transport of fluoride from the plasma to bone tissue, the macroparameter K_{flux}, was calculated as the product of K_i×[$^{19}F^-$] in µmol/[min×cm^3]. The volume of distribution of [^{18}F]fluoride (DV) was determined as K_1/(k_2+k_3). The fraction of tracer in the first tissue compartment that undergoes specific binding to the bone matrix (tBF) was calculated as k_3/(k_2+k_3). For tracer kinetic modelling, a parameter for fractional blood volume (BV) was added to account for non-extracted tracer in the tissue's vascular space. In order to avoid possible identification problems of specific microparameters, the number of fitted parameters was limited to five (K_1–k_4, BV). Due to the specific experimental conditions (standardised tracer injection and automated withdrawal of arterial blood via aortal catheter), the delay in tracer arrival could be set to a fixed value of 0.6 s in each experiment, a mean value that was determined previously [9, 10]. In very few cases, the optimisation routine resulted in negative parameter estimates (i.e. for k_4 or BV) in a particular ROI. In these instances that particular ROI was excluded from further analysis. For fitting of both scans, a weighting factor (1/var) was used to account for the varying amount of statistical noise in the measured data, where var is the variance of the measured activity per pixel per ROI.

Previously, we determined the amount of the [^{18}F]fluoride ion extraction from blood into bone tissue under various flow conditions in normal mini pigs. Assuming that the extraction of [^{15}O]H_2O in a single capillary passage approaches 100%, we were able to show the flow dependency of the [^{18}F]fluoride ion extraction using dual-tracer studies with [^{15}O]H_2O and [^{18}F]fluoride ion PET [10]. The observed relationship between the bone blood flow determined with [^{15}O]H_2O and K_1 in normal mini pigs followed the Renkin-Crone formula [14]:

$$K_1 = f_{H2O} \times E = f_{H2O} \times (1 - e^{(-PS/f_{H2O})}) \quad (1)$$

where E is the so-called unidirectional extraction fraction of the tracer, and PS is the permeability-surface area product and f_{H2O} the arterial flow to the tissue measured by [^{15}O]H_2O. To estimate the "true" regional blood flow (f) from [^{18}F]fluoride ion PET-derived K_1 values, an extraction correction had to be applied. A lookup table of the flow-dependent extraction fraction was generated according to Eq. 1 using the experimentally determined permeability-surface area product of 0.25 (in ml/[min×cm^3]).

The PS product was determined for both groups by a standard non-linear regression fit using data of Fig. 2 and a numerical inversion of Eq. 1. For a known PS product and a measured K_1 the corrected flow (f) is given by the root of:

$$f(1 - e^{(-PS/f)}) - K_1 = 0 \quad (2)$$

Statistical analysis. Unless otherwise indicated, results are expressed as mean values of parameters with their respective standard deviation (SD). Parameters of both groups (PET data and laboratory results) were compared by means of one-way analysis of variance (ANOVA), including tests for homogeneity of group variances using the Bartlett test, selecting a conservative significance level of P≥0.1. The data were then compared by the Tukey studentised range method. In both groups, mean PET parameters were correlated with laboratory results using a non-parametric test (Spearman's rank correlation). A probability of P<0.05 was taken as significant. Statistical tests were performed with the help of the JMP Version 3.2 (SAS, Cary, N.C., USA) statistical software package.

Results

Serum parameters

Laboratory results and cardiocirculatory results during PET scanning are summarised in Table 1. PTH, serum phosphate and 1,25(OH)$_2$-vitamin D levels were significantly higher in gastrectomised animals than in sham-operated animals. Mean age, mean body weight, serum calcium, calcium corrected for albumin (calcium$_{Alb}$), total protein, calcium corrected for protein (calcium$_{Prot}$), albumin, 25-(OH)-vitamin D, haemoglobin and the level of unlabelled fluoride in plasma were not significantly different between groups. Blood gas analysis results (pO_2, pCO_2), mean arterial blood pressure and heart rate were stable throughout both PET scans and not significantly different between gastrectomised and control animals.

Bone blood flow

PET results are summarised in Table 2. Bone blood flow based on [^{15}O]H_2O PET measurements (f_{H2O}) and the

Table 1. Serum, cardiovascular and respiratory parameters obtained 6 months postoperatively in five gastrectomised adult mini pigs and five sham-operated mini pigs

Parameter	Gastrectomy	Sham operation
Fluoride ion in plasma (µg/l)[a]	18.5±2.0	18.4±2.4
Calcium (mval/l)[a]	5.0±0.1	5.4±0.4
$Calcium_{Alb}$ (mmol/l)[a]	5.9±0.1	6.3±0.4
$Calcium_{Prot}$ (mg/dl)[a]	5.1±0.1	5.8±0.4
Phosphate (mmol/l)[a]	2.0±0.1	1.6±0.3*
Alkaline phosphatase (units/l)[a]	129±120	118±74
Parathyroid hormone (pmol/l)[a]	9.0±1.7	6.4±0.9*
25-vitamin D (nmol/l)[a]	27.6±30.4	39.2±13.0
1,25-$(HO)_2$-vitamin D (pmol/l)[a]	759±183	307±131*
Total protein (g/l)[a]	72±6	65±9
Albumin (µmol/l)[a]	568±31	563±40
Hb (mmol/l)[a]	5.2±1.7	5.1±0.7
Arterial PCO_2 (mmHg)[b]	34.0±5.2	33.8±3.4
Arterial PO_2 (mmHg)[b]	244±40	272±40
Heart rate (min^{-1})[b]	91.4±25.8	101.5±15.9
Mean arterial blood pressure (mmHg)[b]	77.9±7.9	73.8±7.7
Age (years)	2.6±1.4	2.5±0.7
Weight (kg)	42.4±14.0	54.7±15.9

Values are means±SD
$Calcium_{Alb}$, calcium corrected for albumin; $Calcium_{Prot}$, calcium corrected for total protein
*$P<0.05$ gastrectomy versus sham-operated
[a] Values obtained at the start of PET scanning
[b] Values obtained during PET scanning

[^{18}F]fluoride ion extraction fraction (E) were not significantly different between gastrectomised and sham-operated animals. Also the volume of distribution (DV_{H2O}) and f, the estimate for bone blood flow derived from PS-corrected K_1 values from [^{18}F]fluoride ion PET, were not different between groups.

Bone metabolism

K_i and K_{flux}, indicators of bone metabolic activity, were significantly increased by approximately 36% and 47%, respectively, after gastrectomy compared with control animals. The parameter k_3 (+110%), reflecting chemisorption and incorporation of [^{18}F]fluoride into the bone matrix, and tBF, the fraction of bound tracer in tissue (+37%), were significantly increased in gastrectomised animals compared with controls ($P<0.05$). All other microparameters (K_1, k_2, k_4), the volume of distribution (DV) and the fractional blood volume (BV) were not significantly different between groups (Table 2).

Relationship between bone blood flow and metabolism

Since bone metabolism was significantly increased after gastrectomy compared with controls while bone blood flow was not different between groups, we further investigated the relationship between blood flow and bone metabolism. Linear regression analysis revealed that bone blood flow (f_{H2O}) and bone metabolism (K_i) were

Table 2. [^{15}O]H_2O and [^{18}F]fluoride ion PET measurements

Parameter[a]	Gastrectomy	Sham operation
[^{15}O]H_2O blood flow f_{H2O} (ml/[min×cm^3])	0.199±0.045	0.181±0.045
[^{18}F]fluoride blood flow estimate f (ml/[min×cm^3])	0.181±0.046	0.176±0.038
[^{15}O]H_2O distribution volume (DV_{H2O}) (ml/cm^3)	0.47±0.05	0.48±0.15
[^{18}F]fluoride ion extraction E (%)	67.2±8.8	74.6±6.0
K_1 (ml/[min×cm^3])	0.131±0.017	0.128±0.017
k_2 (min^{-1})	0.114±0.032	0.115±0.057
k_3 (min^{-1})	0.252±0.047	0.120±0.047*
k_4 (min^{-1})	0.006±0.003	0.004±0.002
Blood volume (BV) (ml/cm^3)	0.025±0.01	0.03±0.018
[^{18}F]fluoride distribution volume (DV) (ml/cm^3)	0.76±0.34	1.16±0.6
Bound fraction of [^{18}F]fluoride in tissue (tBF) (ml/cm^3)	0.71±0.05	0.53±0.06**
K_i (ml/[min×cm^3])	0.091±0.015	0.067±0.015*
K_{flux} (µmol/[min×cm^3])	1.68±0.29	1.14±0.27**

*$P<0.05$ gastrectomy versus sham-operated
**$P<0.02$ gastrectomy versus sham-operated
[a] Parameters include: [^{18}F]Fluoride ion kinetic rate constant estimates (K_1–k_4), fractional blood volume (BV), volume of distribution of [^{18}F]fluoride ion (DV), fraction of bound tracer in tissue (tBF), fluoride influx rate (K_i) and net transport rate of fluoride from the plasma to bone tissue (K_{flux}) of vertebral bodies of mini pigs. Also shown are bone blood flow (f_{H2O}), the volume of distribution (DV_{H2O}) and [^{18}F]fluoride ion extraction (E) measurements based on [^{15}O]H_2O results and estimates for bone blood flow (f) derived from K_1 values using a permeability-surface area product of 0.25 (ml/[min×cm^3]) (see text for details)

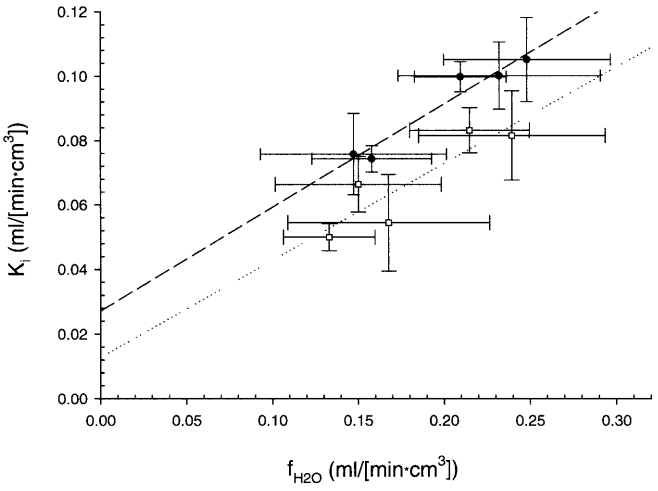

Fig. 1. Relationship between bone blood flow measured by [^{15}O]H_2O PET (f_{H2O}) and bone metabolism measured by [^{18}F]fluoride ion PET (K_i) in vertebral bodies of gastrectomised (*black circles*; *n*=5) and control animals (*white squares*; *n*=5). Regression analyses revealed that bone blood flow (f_{H2O}) and bone metabolism (K_i) were significantly linearly correlated in both groups (gastrectomised animals: y=0.0157+0.32x; adj. r^2=0.93; P<0.001; control animals: y=0.013+0.30x; adj. r^2=0.71; P<0.05)

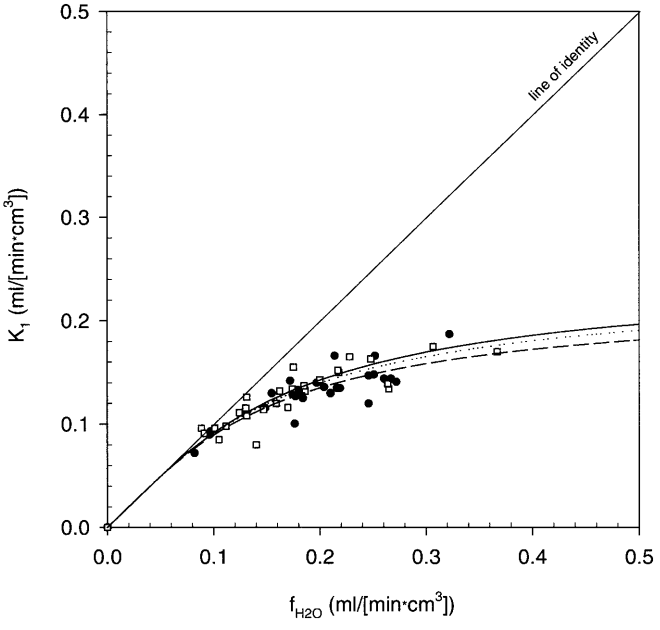

Fig. 2. Regional blood flow measured by [^{15}O]H_2O PET (f_{H2O}) in comparison with corresponding K_1 values derived from [^{18}F]fluoride ion PET in vertebral bodies of gastrectomised (*black circles*; *n*=5) and control animals (*white squares*; *n*=5). The plot displays the pronounced underestimation of the "true" blood flow by K_1 with increasing blood flow in comparison to [^{15}O]H_2O flow results in both groups. The displayed regression line was derived from a group of healthy mini pigs (*n*=7) using the Renkin-Crone formula and the permeability-surface area product (PS) of 0.25 (see text for details). The *dashed line* represents the fitted line to the data of gastrectomised animals (PS=0.23), and the *dotted line* represents the fitted line to the data of the sham-operated animals (PS=0.24)

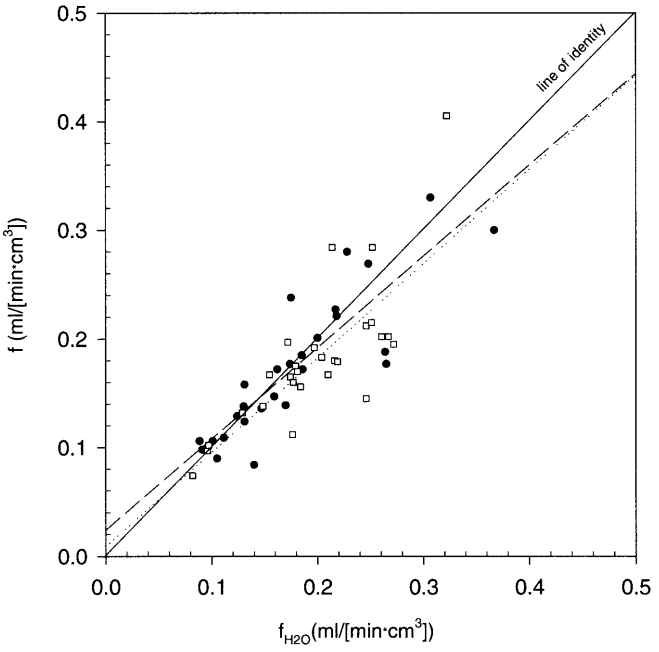

Fig. 3. Relationship between "true" blood flow measured by [^{15}O]H_2O PET (f_{H2O}) and PS product-corrected regional blood flow estimates (f) from [^{18}F]fluoride ion PET derived from individual vertebrae. The PS product correction is followed by a significant improvement of blood flow estimates based on K_1 values in both groups [gastrectomised (*black circles*; *dashed line*; *n*=5) and control animals (*white squares*; *dotted line*; n=5)]. The determined regression lines are not significantly different from the line of identity in either group (gastrectomised animals: y=0.015+0.84x; adj. r^2=0.70; P<0.05; control animals: y=0.013+0.93x; adj. r^2=0.72; P<0.05)

correlated linearly in both groups (gastrectomy: y= 0.027+0.32x; adj. r^2=0.93; P<0.001; controls: y=0.013+ 0.30x; adj. r^2=0.71; P<0.05). These results indicate that bone blood flow and bone metabolism are coupled in high-turnover bone as well as in normal bone tissue. Nevertheless, while the slope of the regression line was almost unchanged in both groups, the intercept with the y-axis was higher in high-turnover bone (Fig. 1). This indicates that the increased bone metabolism is mainly based on an up-regulation of the second step of the [^{18}F]fluoride ion influx, with a consequent increase in the amount of ionic exchange with the bone matrix.

Permeability-surface area product and [^{18}F]fluoride ion extraction

Using the dual-tracer approach with [^{15}O]H_2O and [^{18}F]fluoride ion PET, we investigated the [^{18}F]fluoride ion extraction (E) in relationship to the "true" bone blood flow (f_{H2O}) in both groups. PS product was determined according to Eq. 2 using data from individual ROIs (Fig. 2).

Figure 3 shows f plotted against f_{H2O} both groups. The PS product was determined as 0.24±0.01 in high-turn-

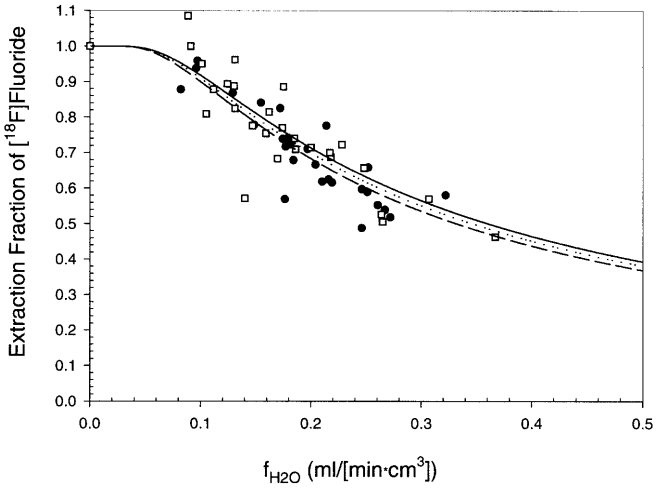

Fig. 4. Relationship between "true" blood flow measured by $[^{15}O]H_2O$ PET (f_{H2O}) and the $[^{18}F]$fluoride ion extraction fraction (E) derived from individual vertebrae. Note the flow-related decrease in E in both groups (*black circles*, gastrectomised animals; *white squares*, control animals). The displayed *solid regression line* represents E derived from healthy mini pigs (see text for details). The *dashed line* represents E derived from gastrectomised animals, and the *dotted line* represents E derived from control animals

over bone and 0.23±0.01 in sham-operated animals (mean ± standard error of estimate in ml/[min×cm^3]). These PS product estimates were not statistically significantly different between the groups. The adjusted correlation coefficient (adj. r^2) of PS was determined to be 0.87 in high-turnover bone and 0.88 in sham-operated animals (P<0.001). Also, the PS product of both groups determined in this study was not significantly different from the PS product previously determined in healthy mini pigs [10]. Using the PS product of 0.25 ml/[min×cm^3] clearly improved blood flow estimations based on K_1 values in normal and high blood flow regions of both groups (compare Figs. 2 and 3). Regression analyses revealed that blood flow estimates (f) were not significantly different from the line of identity in either group (gastrectomy: y=0.015+0.84x; adj. r^2=0.70; P<0.05; controls: y=0.013+0.93x; adj. r^2=0.72; P<0.05).

Since K_1 is the product of blood flow (f) and extraction fraction (E), the quotient of corresponding K_1 and $[^{15}O]H_2O$ blood flow (f_{H2O}) values is an estimate for the regional extraction fraction of the $[^{18}F]$fluoride ion. Figure 4 displays on a regional basis that the $[^{18}F]$fluoride ion extraction fraction (E) is a function of blood flow. We were unable to show any significant differences in the $[^{18}F]$fluoride ion extraction between the groups.

Discussion

The purpose of this study was to investigate the relationship between bone blood flow and bone metabolism in normal and high-turnover bone and to determine whether the capillary permeability and/or surface area is altered in high-turnover bone disease after gastrectomy. We used a well-established mini pig model in which the size of the vertebral bodies is sufficient to ensure that the restricted resolution of dynamic PET studies is not a problem. Also, bone metabolism in mini pigs is similar to that in humans, and the mini pig has been widely used to test new drugs influencing bone metabolism. Most importantly, absolute movement restrictions, as a necessary precondition for the comparison of $[^{15}O]H_2O$ and $[^{18}F]$fluoride ion PET measurements, could be assured by general anaesthesia.

We previously described high-turnover bone disease after gastrectomy in mini pigs using $[^{18}F]$fluoride ion PET [7]. For a detailed description of known changes in bone metabolism after gastrectomy, the reader is referred to the literature [2, 15, 16, 17]. Our previous results as well as a number of other studies support the hypothesis that, owing to disturbances in calcium homeostasis, PTH is increased after gastrectomy, resulting in bone mass loss [2, 6, 7, 18, 19]. We now investigated the relationship between bone blood flow and fluoride ion extraction, since both might be altered in a pathological state like post-gastrectomy high-turnover bone disease.

The uptake of fluoride by bone tissues occurs in several steps. The first stage involves fluoride diffusion from the capillaries into the hydration shells of bone crystallites. These ion-rich aqueous shells are easily accessible to extracellular fluids. From our measurements as well as from other studies, this pool seems to be rapidly exchangeable [10, 20]. With respect to the standard two-tissue compartment model, fluoride enters the unbound tissue compartment. In a second step, fluoride eventually associates with or is incorporated into precursors of hydrofluorapatite and finally into the apatitic lattice itself [20]. In the two-tissue compartment model, these separate biological processes are combined and reflected by the magnitude of the rate constant k_3. Examining our results as well as those of other dynamic $[^{18}F]$fluoride ion PET studies, k_3 seem to be the rate-limiting step of bone metabolism [7, 21]. Apatitic fluoride re-enters the circulating body fluids as a result of the long-term process of bone resorption. Therefore, it seems reasonable that, under normal bone metabolic conditions, the magnitude of the reverse reaction constant k_4 is small. Nevertheless, it has been found previously that the parameter k_4 is needed to account for a small loss of tracer from the bound tissue compartment, which becomes more evident when a prolonged study protocol (120 min) is chosen [9, 13].

As recently published, we found an increase in bone metabolic activity after gastrectomy while bone blood flow estimates based on the permeability-surface area product correction (f) were not different between gastrectomised and control animals [7]. This raised the question of whether (a) the capillary permeability and/or capillary surface area in high-turnover bone disease after gastrecto-

my is altered, or (b) the relationship between bone blood flow and bone metabolism changes under these particular metabolic conditions. Using the dual-tracer approach with [^{15}O]H_2O and [^{18}F]fluoride ion PET, we investigated whether the PS product changes after gastrectomy. These results indicate that the transport of the [^{18}F]fluoride ion across the capillary membrane into the bone tissue and the product of the capillary permeability and surface area is unchanged after gastrectomy. Our results, and those of several other studies, show that there is no evidence that in normal bone the surface area available for exchange responds to an increase in bone blood flow [10, 22]. The discordance between the significantly elevated bone metabolism and unchanged bone blood flow estimates after gastrectomy could be explained by an increase in the fraction of unbound tracer (tBF) in bone tissue undergoing ionic exchange with the bone matrix. Indeed, we found that the microparameter k_3 was significantly elevated after gastrectomy, while the remaining microparameters K_1, k_2 and k_4 were unchanged. Also, calculating tBF, we found a significant increase after gastrectomy compared with controls, while the distribution volume (DV) for [^{18}F]fluoride was not different between groups. Since there was a trend towards an increased k_4 after gastrectomy and tBF does not take into account the magnitude of k_4, tBF slightly overestimates the "true" fraction of bound tracer in bone tissue under these bone metabolic conditions. Nevertheless, our results clearly indicate that the amount of ionic exchange for the [^{18}F]fluoride ion is upregulated in high-turnover bone disease after gastrectomy in porcine bone tissue.

Vertebral bodies consist of a considerable amount of bone marrow. Therefore, tissue inhomogeneity might have influenced PET measurements. Because [^{15}O]H_2O is a freely diffusible tracer, its extraction is instantaneous in both bone and bone marrow. While [^{18}F]fluoride is taken up by the bone tissue and, to a certain extent, permanently bound to the bone matrix, [^{18}F]fluoride is only temporarily present in bone marrow cells. In the event that the tracer extraction of the [^{18}F]fluoride ion (E) is lower in bone marrow than in bone tissue, the bone tissue's extraction fraction would have been underestimated depending on the amount of bone marrow present. However, we consider this possibility rather unlikely because we found a flow-dependent change in the extraction fraction instead of a uniform change. If the presence of bone marrow were the cause of the observed underestimation of blood flow by K_1, then K_1 would underestimate flow at any flow. Instead, we found an extraction fraction close to 100% in low-flow regions, while the extraction fraction decreased progressively with increasing flow. Since the relation of cortical to trabecular bone (containing bone marrow) is relatively stable between different vertebrae of the spinal column, we consider it unlikely that the presence of bone marrow is the cause of the observed relationship between blood flow and [^{18}F]fluoride ion extraction.

Tissue inhomogeneity becomes evident when the distribution volumes of the two tracers are compared. While the distribution into bone marrow is probably comparable for both tracers, the distribution into the remaining bone tissue is different. During the short scanning time of [^{15}O]H_2O PET studies, [^{15}O]H_2O probably only reaches the hydration shells of bone crystallites. On the other hand, during the 2-h [^{18}F]fluoride ion PET scan, a large proportion of [^{18}F]fluoride associates with or is incorporated into the bone matrix. Therefore, it seems reasonable that the distribution volume of [^{18}F]fluoride will be larger than that of [^{15}O]H_2O in vertebrae, as found in this study.

It has long been recognised that bone blood flow and metabolism are coupled in bone tissues under various conditions [8]. In an experimental bone-healing model, bone perfusion was found to be associated with increased uptake of technetium-99m labelled diphosphonates [23]. Due to the restricted resolution in conventional bone imaging, truly quantitative studies, comparing bone blood flow and bone metabolism, are impossible with ^{99m}Tc-labelled diphosphonates. Since the introduction of [^{18}F]fluoride ion PET, the relationship of bone blood flow and metabolism has been investigated using dynamic measurements. Using two-tissue compartmental modelling, a significant correlation was found between K_1 and K_i in various studies [21, 23, 24, 25]. In the light of the flow-dependent reduction of the [^{18}F]fluoride ion extraction, estimation of the bone blood flow based solely on K_1 values can only be performed with acceptable accuracy under low and normal flow conditions. Recently, we used an extraction correction for K_1 values (f) to account for flow-dependent changes in the extraction fraction. A significant correlation between f and the bone mineral apposition rate, and thus the bone formation rate, was found in healthy mini pigs [9].

To our knowledge, this study is the first to investigate bone blood flow and bone metabolism independently using non-invasive techniques. We found a linear correlation between the bone blood flow measured by [^{15}O]H_2O and bone metabolism measured by [^{18}F]fluoride ion PET in both healthy controls and gastrectomised animals with high-turnover bone disease. Currently it is unknown whether this relationship remains unchanged in bone repair after severe trauma or in low-turnover bone disease, for example due to senile osteoporosis. As long as the underlying bone disease does not severely affect the available capillary surface area and/or the capillary permeability for ions, the observed relationship should remain unchanged. We also have to consider possible age- or species-related differences in the [^{18}F]fluoride ion extraction. Therefore, it remains to be determined whether the observed PS product is also valid in humans.

We conclude that the permeability-surface area product of the [^{18}F]fluoride ion is stable in mild to moderate high-turnover bone disease. Therefore, dynamic [^{18}F]fluoride ion PET allows the estimation of bone blood flow

in normal and high-turnover bone, as long as the flow dependency of the extraction fraction is taken into consideration and a proper correction is made for the reduced tracer extraction. Our results indicate that bone blood flow and bone metabolism are coupled in normal bone and high-turnover bone disease after gastrectomy. The up-regulation of the bone metabolism is mainly reflected by an increased ionic exchange of fluoride with the bone matrix.

Acknowledgements. The authors thank the members of the PET facility of the University of Tübingen for their excellent and extensive support. We would also like to thank Prof. Dr. M. Schwaiger for his assistance in preparing the manuscript. This study was supported by DFG (Deutsche Forschungsgemeinschaft) grant No. ZI 415/2-1 and grant No. PI 242/2-1.

References

1. Tovey FI, Hall ML, Ell PJ, Hobsley M. A review of postgastrectomy bone disease. *J Gastroenterol Hepatol* 1992; 7:639–645.
2. Maier GW, Kreis ME, Zittel TT, Becker HD. Calcium regulation and bone mass loss after total gastrectomy in pigs. *Ann Surg* 1997; 225:181–192.
3. Adachi Y, Shiota E, Matsumata T, Iso Y, Yoh R, Kitano S. Osteoporosis after gastrectomy: bone mineral density of lumbar spine assessed by dual-energy X-ray absorptiometry. *Calcif Tissue Int* 2000; 66:119–122.
4. Nihei Z, Kojima K, Ichikawa W, Hirayama R, Mishima Y. Chronological changes in bone mineral content following gastrectomy. *Surg Today* 1996; 26:95–100.
5. Liedman B, Henningsson A, Mellstrom D, Lundell L. Changes in bone metabolism and body composition after total gastrectomy: results of a longitudinal study. *Dig Dis Sci* 2000; 45:819–824.
6. Zittel TT, Zeeb B, Maier GW, Kaiser GW, Zwirner M, Liebich H, Starlinger M, Becker HD. High prevalence of bone disorders after gastrectomy. *Am J Surg* 1997; 174:431–438.
7. Piert M, Zittel TT, Becker GA, Jahn M, Stahlschmidt A, Maier G, Machulla H-J, Bares R. High-turnover osteopenia following gastectomy measured by F-18 fluoride ion positron emission tomography in mini pigs. *J Nucl Med* 2001; 42:339P–340P.
8. Kelly PJ. Pathways of transport in bone. In: Shepherd JT, Abboud FM, Geiger SR, eds. *Handbook of physiology, Sect. 2: The cardiovascular system. Volume III. Peripheral circulation and organ blood flow, part 1.* Bethesda: American Physiological Society; 1983:371–396.
9. Piert M, Zittel TT, Becker GA, Jahn M, Stahlschmidt A, Maier G, Machulla H-J, Bares R. Assessment of porcine bone metabolism by dynamic [^{18}F]fluoride ion positron emission tomography: correlation with bone histomorphometry. *J Nucl Med* 2001; 42:1091–1100.
10. Piert M, Zittel TT, Machulla H-J, Becker GA, Jahn M, Maier G, Bares R, Becker HD. Blood flow measurements with [^{15}O]H_2O and [^{18}F]fluoride ion PET in porcine vertebrae. *J Bone Mineral Res* 1998; 13:1328–1336.
11. Payne RB, Carver ME, Morgan DB. Interpretation of serum total calcium: effects of adjustment for albumin concentration on frequency of abnormal values and on detection of change in the individual. *J Clin Pathol* 1979; 32:32–56.
12. Kety SS. Theory of blood-tissue exchange and its application to measurement of blood flow. *Methods Med Res* 1960; 8:223–227.
13. Hawkins RA, Choi Y, Huang SC, Hoh CK, Dahlbom M, Schiepers C, Satyamurthy N, Barrio JR, Phelps ME. Evaluation of skeletal kinetics of fluoride-18-fluoride ion with PET. *J Nucl Med* 1992; 33:633–642.
14. Renkin EM. Transport of potassium-42 from blood to tissue in isolated mammalian skeletal muscle. *Am J Physiol* 1959; 197:1205–1210.
15. Kocian J, Brodan V. New observations on the absorption of ^{47}Ca in patients with partial gastrectomy. *Digestion* 1975; 12: 193–200.
16. Bisballe S, Eriksen EF, Melsen F, Mosekilde L, Sorensen OH, Hessov I. Osteopenia and osteomalacia after gastrectomy: interrelations between biochemical markers of bone remodelling, vitamin D metabolites, and bone histomorphometry. *Gut* 1991; 32:1303–1307.
17. Rumenapf G, Schwille PO, Erben RG, Schreiber M, Berge B, Fries W, Schmiedl A, Koroma S, Hohenberger W. Gastric fundectomy in the rat: effects on mineral and bone metabolism, with emphasis on the gastrin-calcitonin-parathyroid hormone-vitamin D axis. *Calcif Tissue Int* 1998; 63:433–441.
18. Rumenapf G, Schwille PO, Erben RG, Schreiber M, Fries W, Schmiedl A, Hohenberger W. Osteopenia following total gastrectomy in the rat – state of mineral metabolism and bone histomorphometry. *Eur Surg Res* 1997; 29:209–221.
19. Wojtyczka A, Gorka Z, Bierzynska-Macyszyn G, Rumenapf G, Jonderko K, Schwille PO. Gastrectomy in the rat using two modifications of esophagojejunal anastomosis. General status, local histological changes and relationships to bone density. *Eur Surg Res* 1999; 31:497–507.
20. Whitford GM. Intake and metabolism of fluoride. Adv Dent Res 1994; 8:5–14.
21. Messa C, Goodman WG, Hoh CK, Choi Y, Nissenson AR, Salusky IB, Phelps ME, Hawkins RA. Bone metabolic activity measured with positron emission tomography and [^{18}F]fluoride ion in renal osteodystrophy: correlation with bone histomorphometry. *J Clin Endocrinol Metab* 1993; 77:949–955.
22. McCarthy ID, Hughes SPF. The role of skeletal blood flow in determining the uptake of ^{99m}Tc-methylene diphosphonate. *Calcif Tissue Int* 1983; 35:508–511.
23. Nutton RW, Fitzgerald RH, Kelly PJ. Early dynamic bone imaging as an indicator of osseous blood flow and factors affecting the uptake of ^{99m}Tc-hydroxymethylene diphosphonate in healing bone. J Bone Joint Surg Am 1985; 67:763–770.
24. Berding G, Burchert W, van den Hoff J, Pytlik C, Neukam FW, Meyer GJ, Gratz KF, Hundeshagen H. Evaluation of the incorporation of bone grafts used in maxillofacial surgery with [^{18}F]fluoride ion and dynamic positron emission tomography. *Eur J Nucl Med* 1995; 22:1133–1140.
25. Piert M, Winter E, Becker GA, Bilger K, Machulla H-J, Müller-Schauenburg W, Bares R, Becker HD. Allogenic bone graft viability after revision hip arthroplasty. *Eur J Nucl Med* 1999; 26:615–624.